

CHARACTERIZATION OF INK PIGMENT PENETRATION AND DISTRIBUTION RELATED TO SURFACE TOPOGRAPHY OF PAPER USING CONFOCAL LASER SCANNING MICROSCOPY

Ying Li ^{a, b,*} and Beihai He ^a

The penetration of ink into paper affects the final appearance of printing and the amount of ink usage. In this work, UV-curing fluorescent rose ink was used to investigate the penetration and distribution of the ink pigments as well as their correlation with the surface topography of paper. The ink penetration and distribution were characterized with Confocal Laser Scanning Microscopy (CLSM), whereas the microstructure of the paper surface was observed using Atomic Force Microscopy (AFM). The AFM results showed that the surface of the paper coated with kaolin layer was the smoothest among the samples. Also the pore size of the calcium carbonate coating layer was smaller than that of the kaolin coating layer. Meanwhile, the pore size distribution of the calcium carbonate coating layer appeared to be relatively narrow, compared with other samples. The results of CLSM images indicated that the depth, size, and arrangement of pores affected the penetration depth and distribution of ink pigment on coated paper. The large pores led to deeper penetration of ink pigments, and uniform ink absorption occurred when the pore distribution was uniform. The UV-curing ink pigments not only set on the surface of the uncoated paper, but also they penetrated into the paper interior and adhered to the fiber surface.

Keywords: Coating; Surface topography; Ink pigment penetration; CLSM; AFM

Contact information: a: State Key Laboratory of Pulp and Paper Engineering, South China University of Technology, 510640, Guangzhou, China; b: Faculty of Mechanical and Electrical Engineering, Kunming University of Science and Technology, Kunming, 650093, China; *Corresponding author: haishanying@126.com

INTRODUCTION

Nowadays printing technology has been improved to a substantial degree, and various innovative printing processes have been developed. These developments place very high demands upon ink, paper, and the printing process. Paper's surface topography has a strong influence on its optical and physical properties as well as on the print quality (Lepoutre 1989; Eriksen et al. 2007). Ink penetration and distribution affect the final appearance of printing and ink performance, and they are of primary concern to printers and papermakers with respect to runnability (Aspler and Lepoutre 1991; Glatter and Bousfield 1997; Eriksen and Gregersen 2005). The influence of the coating structure on ink setting rate has been widely investigated (Rousu et al. 2001; Xiang et al. 1998; Donigian et al. 1997). The porosity distribution and surface roughness are the main factors that affect the interaction between printing ink and paper (Preston et al. 2001; Chinga and Helle 2003). The desired optical density on paper is consequentially depen-

dent on the ink absorption by paper, which is determined by structure and optical properties of the paper surface (Havlinová et al. 2000; Desjumaux et al. 2000). Uneven absorption of the ink into paper pores, surface roughness, and complex refractive index variation of the coated paper all contribute to unevenness in gloss and color (Juuti et al. 2007).

Several techniques, e.g., focused ion beam techniques, chromatography, scanning electron microscopy (SEM), and X-ray photoelectron spectroscopy (XPS), have been used to study the distribution of ink components in printed coated and uncoated paper. Eriksen et al. (2007) investigated the influence of newspaper surface roughness on coldset offset ink pigment distribution by SEM. Dalton et al. (2002) explored the distribution of sheet-fed magenta process ink components throughout the printed sheet using secondary ion mass spectrometry, and XPS and showed that the ratio of surface pigment and resin depended on the thickness of the applied film and the coating pore structure. Heard et al. (2004) investigated the distribution of rotogravure cyan ink components in printed coated paper using focused ion beam techniques and showed that the surface topography was of importance, with a smoother and less porous paper having a lower ink demand. Ström and Carlsson (2000) studied the offset ink vehicle separation and absorption of various ink oils into coated paper surfaces by chromatography. Mattila et al. (2002) further investigated the penetration of offset ink resin and oils into uncoated paper by gas chromatography and gel permeation chromatography. Ozaki and Kimura (2000) used the backscattered electron detector on an SEM device to image the distribution of vehicle and pigment in the oxidation cure-type offset ink print and found that the ink vehicle had been dispersed more widely than the ink pigment. Bülow et al. (2002) reported the penetration depth of pigment in paper using heatset offset cyan ink with Cu as a tracer of the colored pigment. Both the lateral pigment distributions and the penetration profiles were found to depend on the size of the pigment grains and the surface treatment of paper. Varjos et al. (2002) tracked the ink vehicle and resin using Cu. Moreover, the factors affecting the ink penetration were identified and the characterizations of the ink components distribution on paper were given qualitatively. Eriksen and Gregersen (2006) found that the average coldset ink pigment penetration increases when the applied printing pressure is increased. However, it was difficult to quantify the degree of penetration of the different components accurately. Meanwhile, in order to acquire the cross-section, the paper must be cut and treated through a complex process. Sometimes the chemical treatments were done to differentiate ink components. These treatment processes may be disadvantageous to accurate observation.

In recent years, Ozaki and Bousfield (2005) investigated three-dimensional characterization of oxidation cure-type ink vehicle penetration and observation of coated paper by staining ink vehicle and binder with fluorescent dye, followed by use of a confocal laser scanning microscope. Rhodamine B was added into neat ink as a probe to stain the ink vehicle; however, not all fluorescent dye was adhered to the oxidation cure-type ink vehicle (Bousfield and Ozaki 2006). Due to some fluorescent dye becoming separated from ink vehicle, the results obtained from CLSM may not represent the true location of the ink vehicle. Nevertheless, this method does avoid the need to cut the paper and embed the sample into the resin to obtain the cross-section. Overall, CLSM has been demonstrated to be a quick, reliable, and effective method for characterizing the three-dimension of coating layer and ink film.

UV-curing ink is distinguished from other type ink in its composition and drying method. UV-curing ink does not involve a solvent and its curing depends on polymerization with the action of photoinitiator. Due to low energy consumption, fast and reliable curing, and low environmental pollution, it can be expected that UV-curing ink will play an important role in the future. There is a need to investigate the penetration and distribution of the UV-curing ink to obtain the information on the interaction between UV-curing ink and paper. Moreover, there has been a lack of reported work observing the three-dimensional distribution of UV-curing ink pigments using CLSM. In this research, the main objective of the experiment was to explore the penetration depth and distribution of UV-curing ink pigment related to the surface topography of paper by CLSM and AFM. UV-curing fluorescent ink pigments were utilized as probes for CLSM to reveal the penetration depth and distribution of the ink pigments.

EXPERIMENTAL

Materials

The basis weight of the woodfree base paper with surface sizing was 68 g/m². The coating layers were composed of kaolin pigment, calcium carbonate pigment, and carboxylic styrene-butadiene latex, which were obtained from suppliers (Mao Ming Clay Company and BASF SD 609ap, China). Sample A and B were coated; however sample C was uncoated. The coating layer components are detailed in Table 1. An ultraviolet curing fluorescent rose ink (Radior France SAS, fluorescent UV 5906) was used for offset printing in this work. The fluorescent pigments are made by staining resin carriers with fluorescent dye. The ink pigment employed an organic fluorescent pigment as a tracer to obtain three-dimensional information of UV-curing ink distribution. The chemical formula for fluorescent dye is given in Fig. 1.

Table 1. Coating Color Recipes

Sample	Kaolin(pph)	Calcium carbonate (pph)	SB(pph)	Solids(%)
A	100	0	10	60
B	0	100	10	60
C	0	0	0	0

Parts per hundred



Fig. 1. Chemical formula of Rhodamine B

Preparation of Laboratory Coated Samples

Coating was carried out with a bar coater (model K303 Multi-coater, RK Print Coat Instruments Ltd, United Kingdom) with a coating speed of 4m/min and a drying temperature of 120 °C for 1 min. The coating thickness was 12 μm , and the coating weight of samples A and B were 18.8 g/m^2 and 21.6 g/m^2 , respectively. The coated samples were uncalendered.

Preparation of Printing Strips

Ink films were applied to the paper strips using a laboratory printing tester (IGT Global standard Tester 2, America) and ink distribution apparatus (IGT Speed Inking Unite 4) with the printing pressure of 625 N and the printing speed of 0.2 m/s. The amount of ink transferred onto the ink distributing roller was 0.2 mL, and the compensation was 0.05 mL every time. UV curing was performed in the presence of oxygen with a prototype UV scanner. One ultraviolet lamp (60 W/cm) was used with a belt speed of 5 m/min.

Measurement of Surface Topography

Atomic force microscopy (AFM) measurements were carried out to characterize the surface microstructure of the paper using a Nanoscope IIIa microscope (Veeco Instruments inc., Santa Barbara, USA). The maps of surface topography were captured with tapping mode in air using standard Si₃N₄ cantilevers. A 10 μm ×10 μm scanning area was chosen to describe the surface microstructure of paper. The roughness of substrates, determined by the scanned area at 10 μm ×10 μm , are often considered to be suitable to describe the surface roughness of paper samples (Kamusewitz and Possart 2003; Tåg et al. 2008), as in the current work. The AFM maps must be treated with flattening order before measurements. Surface plot, depth, roughness and section measurements were carried out using the Nanoscope IIIa image analysis software. The SEM used in this study was an S3700N instrument (Hitachi, Japan). For SEM observation, samples were gold coated and 10 KV beam energy was used to obtain surface topography images in order to reduce the possibility of any thermal damage. The amplification factor was 1000.

Confocal Laser Scanning Microscopy

A Confocal Laser Scanning Microscopy (Leica TCS-SP5) was used to obtain images to reveal the penetration depth and distribution of UV-curing ink pigments. Immersion liquid was supplied by Leica. An X40 oil-immersion objective lens (HC PLAPO, NA 1.25) was chosen. As the laser beam scanned the ink film, the emitted fluorescent light was detected by a photodetector. A confocal beam splitter filter (DD488/543) was used to separate the fluorescent light. The second PMT received He-Ne 543 laser signal, and the detected wavelength ranged from 553 nm to 654 nm. The appropriate focus plane and the best image could be obtained by adjusting the z-directional position, PMT gain, and PMT offset, respectively. Three-dimensional information was gathered as the optical depth images obtained from the scanner. Confocal images were acquired with the XYZ scanning mode in the z direction at intervals of 0.2 μm . A sample was scanned for a period of about 2 to 10 minutes, depending on the thickness of ink film, Z-step, speed, and pixel format of scanning. The

following scanning conditions were selected: pinhole size = 67.95 μm ; digital zoom = 1; scan area = 386 \times 386 μm^2 ; scanning pixel format = 1024 \times 1024; scanning speed = 100 Hz; laser intensity = 70%; Z-step = 0.2 μm ; and excitation wavelength = 543 nm.

RESULTS AND DISCUSSION

Surface Topography of Paper

One of the most important properties of paper is its ability to control the penetration of ink. Surface topography is often critical to ink penetration depth, which plays a major role in determining print gloss, print density, and the appearance of the final printing (Bohuslava et al. 2000). AFM has been used to obtain the three-dimensional characterization of surface topography of paper; and the findings provide the basis for numerical analysis (Udupa et al. 2000). The visual inspection of the topography maps with AFM (seen from Fig. 2) suggests that there were obvious differences among samples A, B, and C. As the AFM tip scans over the surface of paper, the surface depth can be determined, which is defined as the distance from the top of the highest pigment particles to the bottom of the deepest open pores. Topography of AFM maps are color-coded for depth. Pink indicates the highest points and black indicates lowest depths reached by the probe. The surface depth of sample A was 500 nm, and the surface depth of samples B and C were 700 nm and 1500 nm, respectively. Clearly, the surface depth for the paper coated with calcium carbonate pigments was different from the one treated with kaolin pigments, suggesting that the pigment properties indeed affected the pore size and distribution on the surface of coated paper. As can be seen from SEM and AFM images shown in Fig. 2, calcium carbonate pigments (sample B) appeared to be arranged more tightly and orderly than the kaolin pigments (sample A). The trough size of sample B was smaller, and the trough distribution was more uniformly distributed compared with sample A. The section analysis performed on the topography maps gives information on the roughness. It was found that the trough depth of sample B was deeper than that of sample A. Mean-line profile curves of samples are shown in Fig. 2 as well; and the mean roughness (R_a) value over the map of sample A was about 100.3 nm. Figure 2 (b) and (c) show the maps and section analysis for sample B and C. Here the R_a values for topography maps of sample B and C were 167.9 nm and 539.1 nm, respectively. The results showed that there were smaller, deeper, and more troughs on the surface of sample B than those on sample A. In contrast, sample C exhibited the fewest troughs, but the size and depth of the troughs were the largest and deepest.

Figure 3 shows the three-dimensional surface topography maps, from which more direct and detailed surface information can be obtained. As Udupa et al. (2000) pointed out, three-dimensional images provided an obvious indication of peaks and troughs existing on the surface. A comparison of three-dimensional surface images indicated that the topography of samples was significantly different, which could be due to the fact that the nature of the pigments differed and pigments were arranged differently. The troughs of sample C were the largest and deepest as a result of the uncoated surface. It could be concluded from Fig. 3 that sample A was smoother than sample B and sample C.

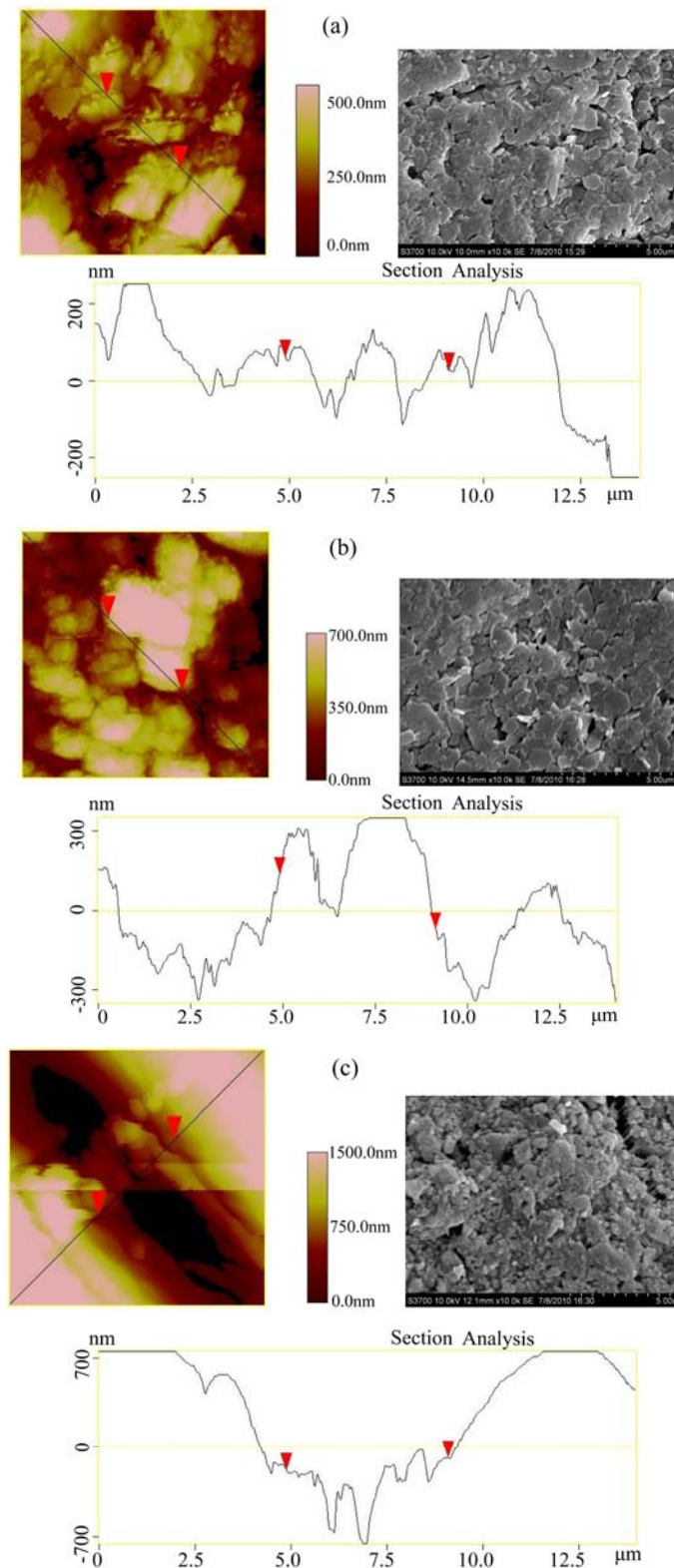


Fig. 2. Topography maps (left on the top), sectional analysis over the straight line showed in the image (below) acquired by AFM (Area: $10\mu\text{m}\times 10\mu\text{m}$) and Surface topography maps acquired by SEM (right on the top) (scale bar: $5\mu\text{m}$). ((a): sample A; (b): sample B; (c): sample C)

Sample C was the roughest of the samples because of that a coating layer on the paper reduces the roughness by filling the depression irregularities of the paper surface (Ström et al. 2003). The smoothness of paper surface depends on the quantity, size, and depth of pores, which in turn is determined by the pigment characteristics or whether the paper has been coated.

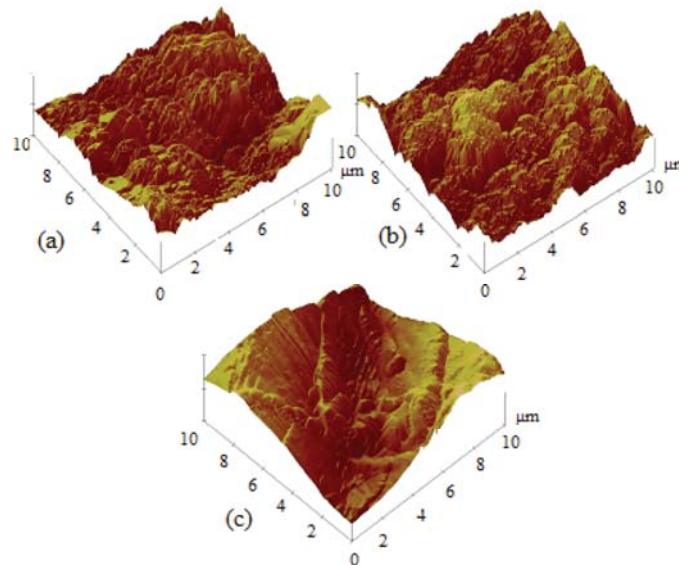


Fig. 3. Three-dimensional topographic maps (Area: $10\mu\text{m}\times 10\mu\text{m}$). Fig. 3 (a), (b), and (c) are the images of sample A, B, and C, respectively.

The depth distributions of topography maps (seen in Fig. 2) are plotted for coordinate data in Fig. 4. The depth distribution maps illustrated the rugged paper surface in the z-direction from numerical characterization (Udupa et al. 2000). Sample A exhibited a narrow distribution, mainly ranging from $0.4\ \mu\text{m}$ to $1.0\ \mu\text{m}$, which is in accordance with the fact that sample A was the smoothest among these samples.

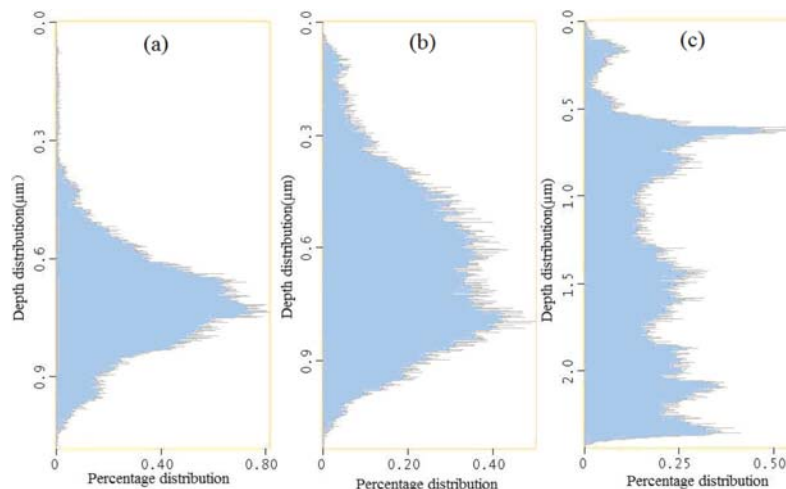


Fig. 4. Depth distribution of topography maps ((a): sample A; (b): sample B; (c): sample C)

As can be seen from Fig. 4, the depth distribution of sample B ranged between 0.2 μm and 1.2 μm , whereas sample C had an even broader depth distribution, ranging from 0.1 μm to 2.5 μm . In other words, the surface of sample B was smoother than sample C. The results demonstrated that the samples behaved differently in terms of the surface structure and the micro smoothness after being coated on the base paper.

Observation of Ink Pigment Distribution from Z-Reconstruction Maps

The fluorescent pigments emitted fluorescence under the stimulation of the He-Ne laser. Three-dimensional images of UV-curing ink pigment penetration and distribution were obtained by reconstructing all XY plane images obtained from CLSM. Figure 5 shows the z-stack images of the paper printed with UV-curing fluorescent rose ink by the XYZ scanning model of CLSM. The green fluorescent regions indicate the presence of ink pigments, and in turn the dark regions represent no absorption or absence of the ink. The results in Fig. 5, i.e., the distribution of fluorescent intensity, showed the uniformity of ink pigments distribution in the z-direction for the samples. Between sample A and sample B, the fluorescent intensity was stronger for sample B, suggesting that the ink layer thickness and distribution of UV-curing ink pigments of sample B were greater and more uniform than those of sample A.

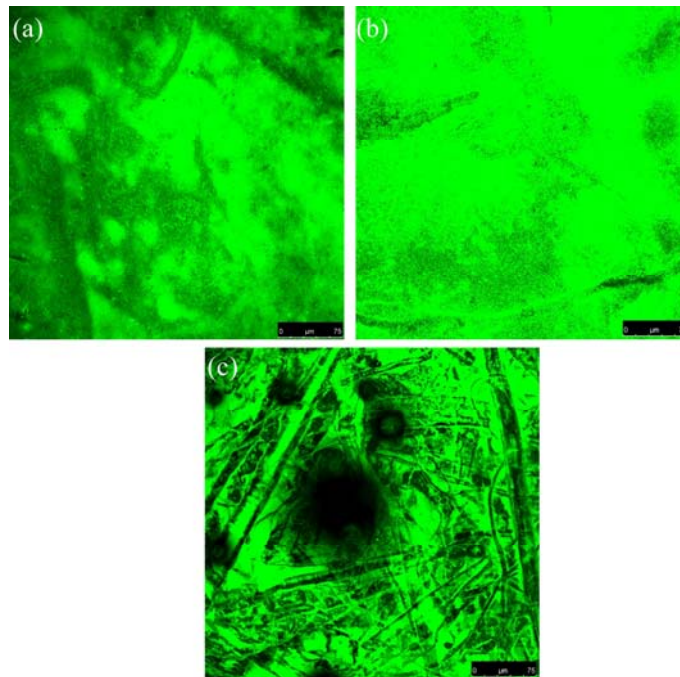


Fig. 5. Z-stack images (scale bar: 15 μm). Fig. 5 (a), (b), and (c) are the images of sample A, B, and C, respectively.

As can be seen from Figs. 2 (b), 3 (b) and 4 (b), there were smaller, deeper, and more uniform troughs on the surface of sample B, compared with sample A, which led to the fast penetration and even distribution of the UV-curing ink transferred onto paper surface. The results were in accordance with the findings from Aspler (1993), i.e., a larger number of smaller pores would make the ink penetrate more rapidly than a smaller

number of larger pores. Sample C was uncoated, so that the roughness value was the highest among all samples, and the troughs distribution was not uniform. As a result, the strongest ink penetration and the most uneven ink absorption were observed in this sample. In this study, UV curing ink pigment were obvious observed from Fig. 5(c), which indicated that UV-curing ink pigments not only set on the surface of the uncoated paper, but also penetrated into paper interior and adhered to the fiber surface.

Characterizing the Ink Pigment Film Thickness

Figure 6 shows the reconstructed images obtained after the samples were measured with the XYZ scanning mode of CLSM in the z direction at intervals of 0.2 μm . The bottom XZ cross-section images were obtained by reconstructing images in the position of line 1. Figure 7 presents the XZ images of ink pigment layer reconstructed from the series of XY sections. Figure 8 and Table 2 summarize the effect of pigment characteristics and coating on the penetration depth and distribution uniformity of ink pigments. The penetration depth of ink pigments in the XZ images (seen from Fig. 7) is also shown in Fig. 8, which was obtained by measuring thirty points at intervals of about 10 μm .

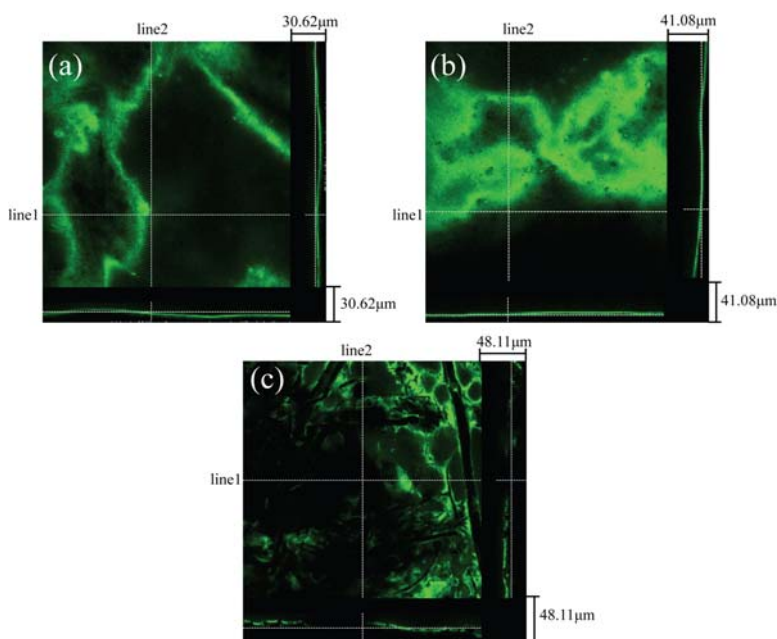


Fig. 6. Reconstructed CLSM images ((a): sample A; (b): sample B; (c): sample C)

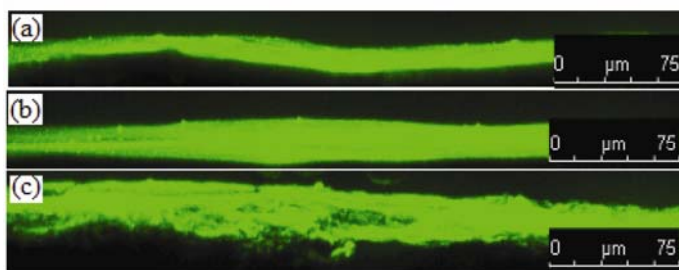


Fig. 7. XZ images of ink pigment layer reconstructed from the series of XY sections (scale bar: 15 μm). Fig. 7 (a), (b), and (c) are the images of sample A, B, and C, respectively.



Fig. 8. Distribution of penetration depth

Table 2. Average Penetration Depth and Standard Deviation

Sample	Average penetration Depth(μm)	Standard Deviation
A	9.72	1.73
B	16.10	2.77
C	24.07	4.32
		n=150

As shown in Fig. 8, the average thickness of ink pigments in sample A was found to be the least among the samples; the deviation of thickness in the X-direction of sample A was also the smallest. The minimum and maximum of the thickness of the ink pigment in sample A were $5.88 \mu\text{m}$ and $12.50 \mu\text{m}$. By contrast, the minimum thickness of ink pigment layer detected for samples B and C were $18.10 \mu\text{m}$ and $19.60 \mu\text{m}$, respectively; correspondingly, the maximum values were $26.90 \mu\text{m}$ and $35.30 \mu\text{m}$. Table 2 lists the average ink film thickness and the standard deviation based on 30 slices detected. Clearly, the average values of ink film thickness and standard deviation of sample A were the smallest among all samples, which indicated that sample A had the lowest ink demand, a finding that can be related to the fact that it has the smoothest surface.

The results could be explained by the images revealed by AFM (seen from Fig. 2, Fig. 3, and Fig. 4). As can be seen from AFM observation, the troughs on the surface of sample B appeared to be smaller, deeper, and more uniform than those on sample A, thus needing the higher amount of ink transferred onto sample B, compared with sample A. Similar results were reported by Heard et al. (2000), i.e., a rougher and more porous paper gave rise to a higher ink demand. Deep troughs led to the deep penetration of ink pigments, and uneven trough distribution resulted in uneven ink absorption. The deeper penetration and uneven setting of ink pigments are undesirable, tending to induce the back-trap mottle and decrease the gloss of printing. The smooth surface of paper improves print quality and decrease the amount of ink usage. In terms of the results shown in this work, sample C is less desirable because it yielded the thickest ink film and the most uneven ink distribution, factors which lead to significant printing defects.

CONCLUSIONS

1. Investigation into the penetration depth and distribution of UV-curing ink pigments could be effectively conducted with Confocal Laser Scanning Microscopy (CLSM). With this technique, the quantitative analysis in the penetration depth of UV-curing ink pigments is achieved, and the accuracy of measurement could reach 10 nm in our research.
2. Kaolin pigments arrange themselves more tightly than calcium carbonate pigments on the coating surface. The roughness of a calcium carbonate coating layer tends to be higher than that of a kaolin coating layer, but the troughs distribution of calcium carbonate coating layer appear to be more even, compared with the kaolin coating layer. The troughs of uncoated paper are the largest and deepest.
- 3 It can be concluded that deeper troughs on the paper surface lead to the deeper penetration of UV-curing ink pigments, and uneven troughs distribution will result in uneven ink absorption. The average values of penetration depth and standard deviation of kaolin coating paper were the smallest among the samples, and kaolin coating paper had the lower ink demand compared with calcium carbonate coating paper, which can be related to the smoother surface, so a smoother and much less porous paper sheet results in a lower ink demand.

REFERENCES CITED

- Aspler, J. S. (1993). "Interaction of ink and water with paper surface in printing: A review," *Nordic Pulp Paper Res. J.* 8(1), 68-74.
- Aspler, J. S., and Lepoutre, P. (1991). "The transfer and setting of ink on coated paper," *Progress in Organic Coatings* 19(4), 333-357.
- Bülow, K., Kristiansson, P., Tullander, E., Östling, S., Elfman, M., Malmqvist, K., Pallon, J., and Shariff, A. (2002). "The penetration depth and lateral distribution of pigment related to pigment grain size and the calendering of paper," *Nuclear Instruments and Methods in Physics Research. B* 189, 308-314.
- Bohuslava H., L'udmila H., Vlasta B., Zuzana L., Juraj K., and Viera J. (2000). "Ink receptivity on paper-characterization of paper materials," *Colloids Surf. A* 168, 251-259.
- Chinga, G., and Helle, T. (2003). "Relationships between the coating surface structural variation and print quality," *Journal of Pulp and Paper Science.* 29(6), 179-184.
- Dalton, J. S., Preston, J. S., Heard, P. J., Allen, G. C., Elton, N. J., and Husband, J. C. (2002). "Investigation into the distribution of ink components throughout printed coated paper: Part 2: Utilising XPS and SIMS," *Colloid Surf. A-Physicochem. Eng. Asp.* 205(3), 199-213.
- Desjumaux, D. M., Bousfield, D. W., Glatter, T. P., and Van Gilder, R. L. (2000). "The influence of latex type and concentration on ink gloss dynamics," *Progress in Organic Coatings* 38(2), 89-95.
- Donigian, D. W., Ishley, J. N., and Wise, K. J. (1997). "Coating pore structure and offset printed gloss," *TAPPI J.* 80(5), 163-172.

- Eriksen, Ø., Johannesen, E., and Weiby Gregersen, Ø. (2007). "The influence of paper surface roughness on ink pigment distribution," *Apptia. J.* 60(5), 384-389.
- Eriksen, Ø., and Weiby Gregersen, Ø. (2005). "The influence of ink pigment penetration and paper structure on print through," *Nordic Pulp Paper Res. J.* 20(2), 242-246.
- Eriksen, Ø., and Weiby Gregersen, Ø. (2006). "Ink pigment location measured as the position of clay in yellow coldset ink," *Nordic Pulp Paper Res. J.* 21(4), 460-465.
- Glatter, T. P., and Bousfield, D. W. (1997). "Print gloss development on a model substrate," *TAPPI J.* 80(7), 125-132.
- Havlíková, B., Horňáková, L., Brezová, V., Liptáková, Z., and Kindernay, J. (2000). "Ink receptivity on paper-characterization of paper materials," *Colloids Surf. A* 168, 251-259.
- Heard, P. J., Preston, J. S., Parsons, D. J., and Allen, G. C. (2004). "Visualization of the distribution of ink components in printed coated paper using focused ion beam techniques," *Colloids Surf. A* 244, 67-71.
- Juuti, M., Prikäri, T., Alarousu, E., Koivula, H., Mylly, M., Lähteelä, A., Toivakka, M., Timonen, J., Myllylä, R., and Peiponen, K. E. (2007). "Detection of local specular gloss and surface roughness from black prints," *Colloids Surf. A* 299, 101-108.
- Kamusewitz, H., and Possart, W. (2003). "Wetting and scanning force microscopy on rough poly surfaces: Wenzel's roughness factor and the thermodynamic contact angle," *Appl. Phys. A* 76, 889-902.
- Lepoutre, P. (1989). "The structure of paper coatings: An update," *Progress in Organic Coatings*. 17(2), 89-106.
- Mattila, U., Tahkola, K., Nieminen, S., Kleen, M. (2002). "Penetration and separation of ink resin and oils in uncoated paper studied by chromatographic methods," *Proc. Intl. Printing Graphic Arts Conf., ATIP. (III)*, 1-9.
- Ozaki, Y., Bousfield, D. W., and Shaler, S. M. (2005), "Three-dimensional characterization of ink vehicle penetration by laser scanning confocal microscopy," *Journal of Pulp and Paper Science*. 31(1), 48-52.
- Ozaki, Y., Bousfield, D. W., and Shaler, S. M. (2006). "Three-dimensional observation of coated paper by confocal laser scanning microscopy," *TAPPI J.* 5(2), 3-8.
- Ozaki, Y., and Kimura, M. (2000). "Visualisation of printing ink vehicle on paper surfaces by a SEM technique," *Apptia J.* 53(3), 216-219.
- Preston, J. S., Elton, N. J., Legrix, A., and Nutbeem, C. (2001). "The role of pore density in the setting of offset printed ink on coated paper," in: *Proceeding of TAPPI Advanced Coating Fundamentals Symposium, San Diego, May 2001*.
- Rousu, S., Gane, P. A. C., and Speilmann, D. (2001). "Separation of off-set ink components during absorption into pigment coating structures," *Nordic Pulp Paper Res. J.* 15(5), 527-535.
- Ström, G., Englund, A., and Karathanasis, M. (2003). "Effect of coating structure on print gloss after sheet-fed offset printing," *Nordic Pulp and Paper Research J.* 18(1), 108-115.
- Ström, G., Gustafsson, J., and Sjölin, K. (2000). "Separation of ink constituents during ink setting on coated substrates," *IPGAC, Savannah, USA, 2000*.
- Tåg, C. M., Juuti, M., Peiponen, K. E., and Rosenholm, J.B. (2008). "Print mottling: Solid-liquid adhesion related to appearance," *Colloids Surf. A* 317, 658-665.

Udupa, G., Singaperumal, M., Sirohi, R. S., and Kothiyal, M. P. (2000).

“Characterization of surface topography by confocal microscopy II: The micro and macro surface irregularities,” *Measurement Science Technology*.11, 315-329.

Vajos, p., Kataja, K., Lipponen, M. and Leino, P.Q.(2002). “Absorption studies of coldset ink components into paper,” 11th International Printing and Graphics Arts Conference, Vol.1, Bordeaux Lac, France, Paris.

Xiang, Y., Desjumeaux, D., Bousfield, D., and Forbes, M. F. (1998). “The relationship between coating layer composition, ink setting rate and offset print gloss,” Preprints of the Pan Pacific and International Printing and Graphic Arts Conference, Quebec, 85-91.

Article submitted: November 20, 2011; Peer review completed: January 11, 2011;

Revised version received: January 31, 2011; Revised version accepted: May 24, 2011;

Published: May 26, 2011.